

## Technical Note SCD 1

# Comparison of CCD Detectors and Image Plates

Image Plates became the most popular detectors for macromolecular crystallography after their introduction by Miyahara in 1986<sup>1</sup>. However, CCD-based detectors (Figure 1) have almost entirely replaced Image Plates at synchrotron beam lines<sup>2</sup> and are now increasingly being applied in home laboratory applications as well<sup>3</sup>.

The rapid improvement in CCD technology over the last several years has now yielded detectors with decisive advantages when compared to Image Plates including significantly higher sensitivity, better spatial resolution and faster readout times.

Because of these advantages, state-of-the-art CCDs can produce significantly superior data quality in a fraction of the time required for conventional Image Plates<sup>3, 4</sup>.

### Characterization of X-ray Detectors

To understand the relative advantages and disadvantages of Image Plate and CCD detectors it is useful to review the parameters used to characterize the performance of X-ray detectors in general.

The most important performance characteristics of a detector are its sensitivity, dynamic range, resolving power and readout deadtime.

#### Sensitivity

Sensitivity is most often quantified by the Detective Quantum Efficiency (DQE). DQE is the ratio of the sensitivity of the detector to an ideal, photon-counting detector<sup>4,5</sup>. For example, a detector with a DQE of 1.0 is equal in sensitivity to an ideal detector, while a detector with a DQE of 0.5 is half as sensitive as an ideal detector (and would thus require approximately twice as long to acquire a data set with equivalent statistics).

It should be understood that the DQE is not a scalar quantity but depends of the intensity of the Bragg reflection. All analog detectors (which include both CCDs and Image Plates) exhibit higher DQE for strong reflections.

The DQE of an integrating detector in general can be written as:

$$DQE = \frac{T_w \eta_{ph}}{1 + 1/g + \frac{A(n_r^2 + i_d t)}{IT_w g^2}}$$

$T_w$  = transmission efficiency of the X-ray window

$\eta_{ph}$  = absorption efficiency of the phosphor screen

$g$  = quantum gain of the detector (the number of detected electrons per each incident X-ray)

$A$  = the area of a Bragg reflection (in pixels)

$i_d$  = dark current.

For strong reflections the DQE reduces to:

$$DQE_{strong} \cong \frac{T_w h_p}{1 + 1/g}$$

Therefore, to efficiently record the strong reflections it is important for the detector to have a high window transparency,  $T_w$ , good x-ray absorption,  $\eta_{ph}$ , and a high quantum gain,  $g \gg 1$ .

For weak reflections the DQE reduces to:

$$DQE_{weak} \cong \frac{IT_w^2 g^2 \eta_{ph}}{n_{tot}}$$

where  $n_{tot}$  is the total noise of the detector (that is, the combination of readout noise and dark current noise).

Therefore, to accurately record the weakest reflection it is important for the detector to exhibit high window transparency, high X-ray absorption efficiency, high quantum gain and low total detector noise.

### Dynamic range

Dynamic range quantifies the largest signal that can be recorded before saturation of the detector relative to the smallest signal that can be distinguished above the noise floor<sup>4</sup>. That is,

$$DR = \frac{I_{max}}{I_{min}}$$

Most often, the minimum detectable signal is comparable to the noise floor and thus the dynamic range can be written approximately as:

$$DR = \frac{I_{max}}{n_{tot}}$$

To record the entire Bragg diffraction pattern it is necessary for the dynamic range of the detector to at least be equal to the range of reflection intensities of the sample of interest. In practice, a dynamic range of  $10^4$  is sufficient for most macromolecules. However, larger dynamic range is useful in that it makes it less critical to select the optimal exposure time for the experiment.

### Resolving power

The resolving power of the detector,  $P_{res}$ , quantifies the ability to achieve (near) atomic resolution data for samples with large unit cells without changing the  $2\theta$  position of the detector. The resolving power is approximately given by the size of the detector normalized by the point spread function

$$P_{res} = \frac{D_{det}}{d_{PSF}}$$

where  $D_{det}$  is the linear size of the detector and  $d_{PSF}$  is the point spread function (full width at half maximum). Thus, the resolving power of a large detector with a modest point spread function would be similar to that of a smaller detector with higher spatial resolution.

### Readout Time

Finally, the readout deadtime is the time during which the X-ray beam must be shuttered off in order to read out the integrated signal in the detector. While low readout deadtime is an advantage in almost any experiment, it is particularly critical for those using high intensity sources such as synchrotron beamlines and the latest generation of laboratory microfocus rotating anode generators (which can rival the intensity of second generation synchrotron beamlines).

## Operational Principles and Characteristics of Image Plates

The operational principle of an Image Plate is shown schematically in Figure 2. The heart of the Image Plate is a storage phosphor screen. When the storage phosphor is exposed to X-rays, secondary electrons are trapped in so-called metastable F-centers (Figure 1). The number of F-centers produced is proportional to the X-ray energy. The most common storage phosphors are the barium fluorohalides (mixtures of BaF and BaBr or BaI) which have a conversion gain (number of F-centers produced per unit energy of the incident X-rays) on the order of 8 F-centers per keV<sup>6</sup>. So for an 8.1 keV X-ray (Cu K $\alpha$ ), approximately 64 metastable F-centers are produced for each incident X-ray.

Figure 1

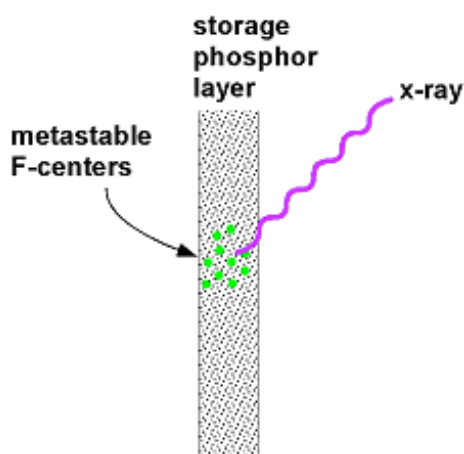
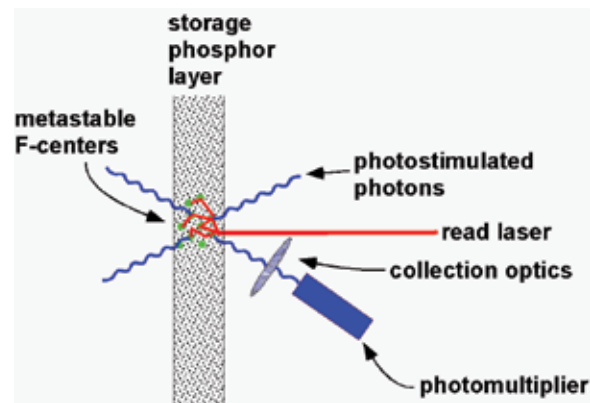


### Image plate design

After the exposure, these metastable centers can be excited by a read laser to release visible photons in a process known as photostimulation or bleaching (Figure 3). These photostimulated photons can then be detected by an appropriate detector (typically a photomultiplier tube with a multilayer filter to reject the scattered read laser light). By scanning the laser across the surface of the plate it is thus possible to determine the integrated number of X-rays incident at each location.

Figure 2



An incident X-ray produces metastable F-centers in a storage phosphor screen. A read laser excites the metastable F-centers to emit photostimulated photons (whose intensity is proportional to the original incident X-ray flux).

The bleaching process only reads a fraction of the metastable F-centers. The fraction of F-centers bleached is a function of the intensity of the probe laser, its wavelength and the dwell time. In principle, with sufficiently long dwell times it is possible to approach 100% bleaching efficiency<sup>6</sup>. However, in this case the readout of the plate would be impractically long (many minutes per frame). For typical laser intensities and dwell times on the order of several tens of microseconds, bleaching fractions on the order of 10-30% are achieved<sup>6</sup>.

Since the plate is not completely bleached after the readout, the plate will still contain active metastable F-centers that could be bleached on subsequent frames (thus causing "ghost" images). To completely erase the remaining, unbleached F-centers after the plate is read it is exposed to an intense, broadband light source for some tens of seconds<sup>6</sup>.

The biggest advantage of this scheme is that it allows a relatively large active area to be achieved inexpensively and Image Plates are thus the largest commercially available X-ray imagers with active areas of up to 345 mm diameter.

Another advantage is that the storage phosphor plates exhibit a relatively large dynamic range, typically greater than 100,000. Until recently, Image Plates had by far the largest dynamic range of commercially-available X-ray imagers. However, recently CCD detectors have become available that rival the dynamic range of Image Plates.

Together, the large active area and dynamic range mean that the Image Plate can record the entire Bragg diffraction pattern of most samples without saturation. It is these valuable properties that have made Image Plates a popular choice for home laboratory macromolecular crystallography.

However, the Image Plates also have a number of features that are much less desirable. Perhaps their biggest disadvantage is their relatively long readout times. Because of the long lifetimes of the F-center excited states it typically takes several tens of microseconds to bleach each pixel on the image plate<sup>6</sup>. Because of this relatively long dwell time for each pixel, the total readout time for the entire plate is typically on the order of 1 to 2 minutes (with an additional 30 seconds to erase the plate). This long readout cycle is a serious disadvantage in experiments at synchrotron beamlines where integration times are typically on the order of seconds or less and where Image Plates, therefore, achieve an unacceptably low duty cycle. Indeed, the poor duty cycle of Image Plate detectors motivated the original development of CCD detectors (which have much shorter readout times and have therefore essentially replaced Image Plates at synchrotron beamlines<sup>7</sup>).

In recent years, high end home laboratory sources have become sufficiently intense so as to rival second generation synchrotron beamlines<sup>14</sup> and thus, the long readout time of Image Plates is becoming an increasing disadvantage for home lab sources as well. In order to minimize this disadvantage, Image Plate designs may employ two or three Image Plates on a belt so that one Image Plate can be readout while the other is exposed. This can reduce the effective deadtime between frames to the belt interchange time (typically of order 10 seconds). However, this decrease in deadtime is achieved only if the exposure time for each frame is longer than the plate readout time. Therefore, Image Plates can not acquire a series of short (<1 minute) exposure time frames as is required for efficient data capture on synchrotron beamlines (and increasingly on ultra-intense laboratory sources).

The other principle disadvantage of the Image Plate is its relatively modest sensitivity. As noted above, the sensitivity of a detector can be characterized by its Detective Quantum Efficiency (DQE).

For the detector to exhibit a high DQE it must have a high quantum gain, that is,  $g \gg 1$ .

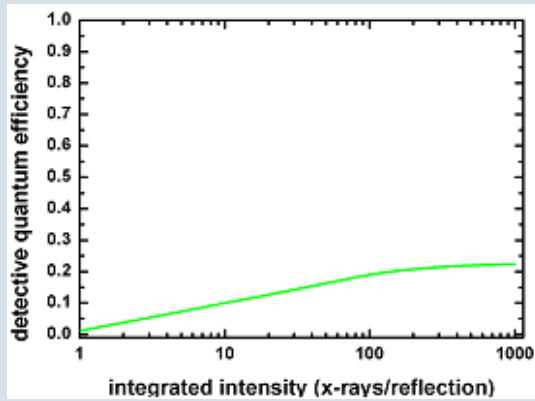
In the case of an image plate, the quantum gain can be written:

$$g = g_F \eta_{bl} \eta_{op} QE_{pm}$$

where  $g_F$  is the number of metastable F-centers per incident X-ray,  $\eta_{bl}$  is the bleaching efficiency (that is, the fraction of metastable F-centers actually photostimulated by the read laser),  $\eta_{op}$  is the collection efficiency of the collection optics and  $QE_{pm}$  is the quantum efficiency of the photo-multiplier tube. As noted above, for Ba(F,Cl) phosphors the primary gain,  $g_p$  is of order 64 F-centers/X-ray (at 8.1 keV). The bleaching efficiency,  $\eta_{bl}$ , is determined by the laser power and the dwell time but is typically on the order of 0.2-0.3, the optical collection efficiency,  $\eta_{op}$ , is typically on the order of 0.2 and the quantum efficiency of the photomultiplier is typically on the order of 0.15 (for a multi-alkali photocathode).

Thus, the overall quantum gain of a typical Image Plate for Cu K $\alpha$  X-rays is  $g = 64 * 0.3 * 0.2 * 0.15 = 0.6$  electrons/X-ray. Because of this relatively low quantum gain Image Plates achieve relatively modest DQEs as shown in Figure 3. It can be seen that for strong reflections, the typical Image Plate is four times less sensitive than an ideal detector while for weaker reflections (<10 X-rays/reflection), the Image Plate is more than ten times less sensitive.

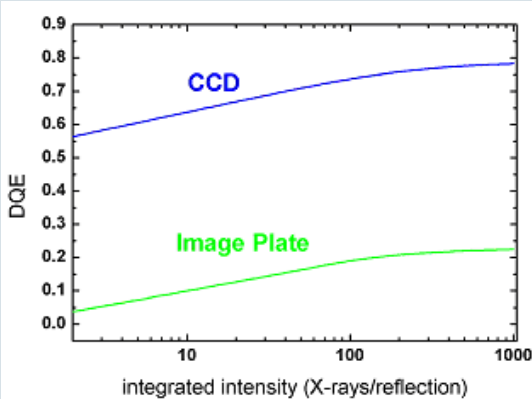
Figure 3



The calculated DQE for a typical Image Plate detector.

As seen in Figure 4, the DQE of a typical image plate is also significantly lower than the DQE of a comparable CCD detector.

Figure 4



The DQE for a typical Image Plate compared to a modern CCD detector. Note that the CCD is approximately three times more sensitive than the Image Plate for strong reflections (>100 X-rays per reflection) and more than ten times more sensitive for weak reflections (<10 X-rays/reflection).

## Operating Principles and Characteristics of CCDs

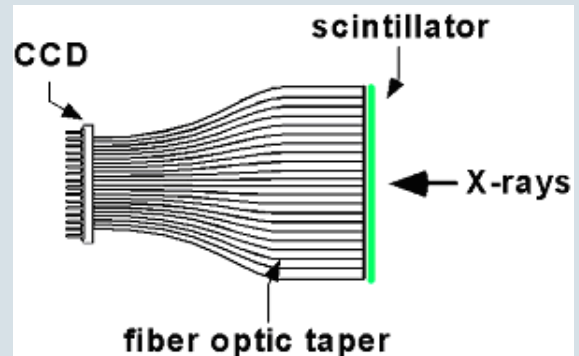
As noted above, CCD-based detectors were developed in order to address the operational deficiencies of Image Plates, namely long readout times and low sensitivity. Modern CCD detectors have readout times more than 100 times faster than Image Plates and sensitivity more than three times higher<sup>8</sup>.

Together, these advantages allow CCDs to achieve superior data quality in a fraction of the time required to acquire comparable data using an Image Plate.

The operating principle of a CCD is shown in Figure 5. The X-rays excite a scintillator screen to produce visible photons. These photons are focused onto a CCD imager where they create electron-hole pairs. The electrons are stored in potential wells at each pixel site and then are read out by applying appropriately phased voltages to the gate electrodes on the CCD.

A great advantage of this scheme is that CCDs can be read out much faster than Image Plates (modern CCDs can be readout in less than one second for an entire frame). Again, this is about two orders of magnitude faster than an Image Plate with comparable resolution.

Figure 5



Operating principle of a CCD-based X-ray detector. X-rays excite a phosphor screen, producing visible photons which are focused onto a CCD imager using a fiber optic taper.

The other significant advantage of the CCD is that the sensitivity is much higher than an Image Plate due to its significantly higher quantum gain.

The quantum gain of a CCD can be written as:

$$g_{CCD} = g_{phosphor} \eta_{optics} QE_{CCD}$$

where  $g_{phosphor}$  is the gain of the phosphor screen (that is, the number of visible photons produced for each incident X-ray, typically on the order of 350 for a Cu  $K\alpha$  X-ray),  $\eta_{optics}$  is the transmission efficiency of the coupling optics (typically of order 0.3 for 1.5 demagnification) and  $QE_{CCD}$  is the quantum efficiency of the CCD (typically of order 0.3). In this example, the quantum gain of the CCD detector would be on the order of  $g_{CCD} = 350 \times 0.3 \times 0.3 = 30$ . Thus, the typical quantum gain of a CCD detector is more than an order of magnitude larger than the Image Plate. This in turn allows the CCD to achieve a significantly higher DQE than the Image Plate.

What this means in practice is that the CCD can achieve comparable data quality about three times faster than an Image Plate for strongly diffracting samples and about 10 times faster than the Image Plate for weakly diffracting samples.

Or, if the time for the experiment is fixed, the CCD will produce significantly superior data quality compared to the Image Plate.

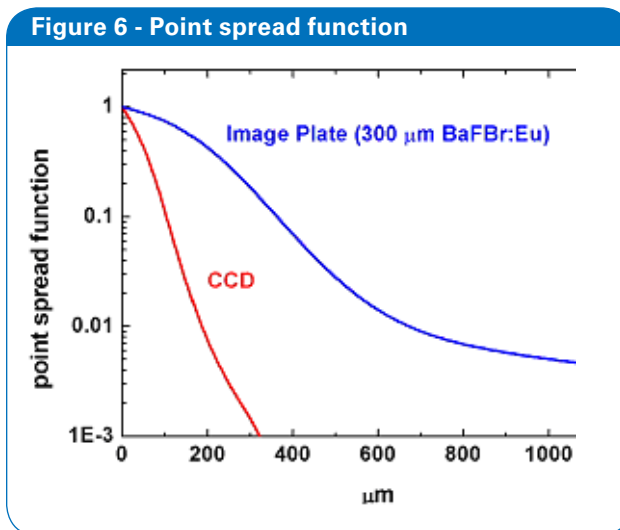
## Size, Point Spread Function and Resolution

One of the most obvious differences between CCD detectors and Image plates is the physical size of the imaging area. Image Plates typically are designed with active areas of the order of up to 450 mm (diagonal) while the largest available CCD imagers are only about 200 mm (diagonal).

It is possible to tile several CCD detectors into a mosaic that is as large as a typical image plate. However, such CCD mosaics are rather expensive compared to an Image Plate and thus while this type of mosaic finds routine applications at synchrotron beamlines its cost is prohibitive for most home laboratory applications.

Rather, for home laboratory instruments a single CCD module with a size on the order of 130 mm diagonal is typically used. Though this is significantly smaller than a typical Image Plate, in many cases the better point spread of the CCD allows it to be moved closer to the sample in order to achieve the same resolution as the larger Image Plate<sup>9</sup>.

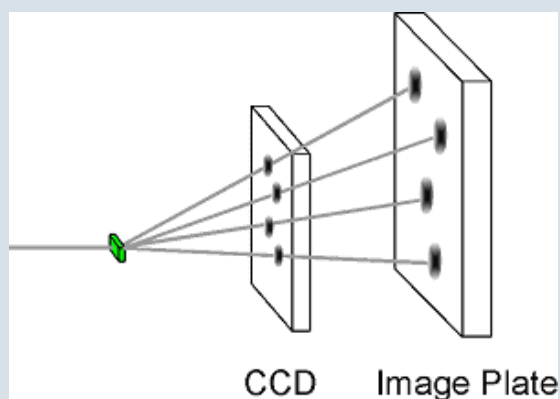
Figure 6 shows the measured point spread function for a CCD detector (optimized for Cu  $K\alpha$  radiation) and an Image Plate<sup>9</sup>. Note that the CCD typically achieves a point spread function that is more than two times better than the Image Plate. The relatively poor point spread of the Image Plate is primarily due to the scatter of the read laser light in the storage phosphor screen<sup>9</sup>.



Comparison of the point spread function of a CCD and an Image Plate. The CCD achieves significantly higher spatial resolution than the Image Plate.

Because of its better point spread function, the CCD can be operated closer to the sample without suffering overlapping reflections (as long as the mosaic spread of the diffracted beam is smaller than point spread of the detector) as shown schematically in Figure 7.

Figure 7 - Schematic



Because of its higher spatial resolution the CCD can be operated closer to the sample and thus achieve a comparable resolution to an Image Plate despite its smaller physical size.

Table 1 shows that a smaller CCD (130 mm diagonal) running at a typical sample to detector distance of 40 mm can achieve comparable resolution to a much larger Image Plate (420 mm diagonal) running at a larger sample to detector distance (100 mm).

Table 1 - Coverage comparison

	CCD	Image Plate
Size (diagonal, mm)	130	420
Point spread	80	200
Typical operating distance (mm)	40	100
Resolution at edge of detector (Å), $2\theta=0$	1.78*	1.63**
Resolution at edge of detector (Å), $2\theta=\max$	0.99*	0.93**

\*at 40 mm sample to detector distance.

\*\*at 100 mm sample to detector distance.

## Experimental Comparison Between CCDs and Image Plates

Surprisingly few direct comparisons between CCD detectors and Image plates have been published but all the available published comparisons strongly support the operational superiority of CCDs as described theoretically above.

A.M. Deacon et al. published a study of Concanavalin A conducted at the SRS in Daresbury<sup>10</sup>. In both cases the data was acquired to the same resolution (0.94 Angstroms) in the same amount of time. In this case the CCD was able to deliver significantly superior data quality: the overall  $R_{\text{merge}}$  for the CCD was 13% compared to 44% for the Image Plate. S. Muchmore published a comparison of a CCD and an Image Plate in the home laboratory. In this case, HEW Lysozyme data were acquired to a resolution of 1.8 Angstroms. He found that it took the Image Plate four times longer to acquire data with comparable quality to that collected with the CCD. Even then, the CCD data in the highest resolution shell had a much lower  $R_{\text{merge}}$  value<sup>3</sup> (CCD  $R_{\text{merge}}=17\%$ , IP  $R_{\text{merge}}=22\%$ ).

In addition to these crystallographic comparisons, CCDs have also been compared to Image Plates in other scientific and medical X-ray imaging applications.

J. Howe et al. have compared the performance of CCD and Image Plates as detectors for X-ray spectroscopy and reported that for weak signals, the CCD exhibited more than five times higher sensitivity and noted that the "CCD camera is by far the most suitable detector, offering much greater signal-to-noise ratio and sensitivity"<sup>11</sup>.

Finally, R. Schulz-Wendtland et al. compared the performance of Image Plates and CCDs for digital mammography. He again reports that the CCD produced the best data quality<sup>12</sup>.

These studies are consistent with the DQE calculations presented above and confirm that CCD-based detectors can acquire data of comparable quality much faster than an Image Plate or, in the same period of time deliver significantly superior data quality.

## Operational Advantages of CCDs

One of the most common applications of CCDs in the home lab is crystal screening before a trip to a beamline facility. Here the advantage of the CCD is obvious: several crystals can be completely characterized on the CCD during the time an Image Plate would require to integrate and readout its first exposure.

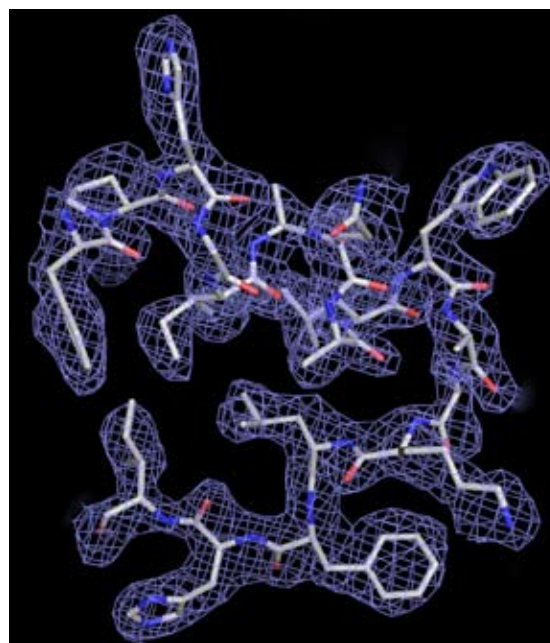
Perhaps a less obvious advantage of the fast readout of CCDs is fine-slicing and high redundancy for improving data quality.

Because of the relatively slow readout of Image Plate detectors, they are typically used in wide-frame mode. That is, each frame of data is typically integrated over 1-2 degrees in  $\phi$ . This reduces the number of readout cycles required by the Image Plate. However, for crystals whose mosaic spread is smaller than 1 degree there is a significant advantage in running in narrow frame or fine  $\phi$ -slicing mode where a frame would be integrated over only 0.3-0.5 degrees (or less)<sup>8</sup>. In fine slicing integration there is less scattered X-ray background superimposed on each X-ray reflection and thus higher data accuracy can be achieved. This is especially important for samples with a high scattered X-ray background or small samples. The very fast readout of CCDs makes them ideal for fine sliced data acquisition.

Another case where the high sensitivity and fast readout of the CCD provide a distinct advantage is in acquiring data sets with high redundancy. It is well known that collecting data with high redundancy reduces both statistical and systematic errors and thus allows significantly higher data quality. This is especially important, for example, in SAD phasing experiments from native sulphur where extracting the weak anomalous signal requires very high data quality.

Data quality has a big impact on the success of SAD phasing experiments, particularly when the anomalous signal is small. A good example is the sulfur-SAD phasing of Glucose Isomerase from *Streptomyces rubiginosus*. This 43 kDa enzyme contains 388 residues including eight methionines and one cysteine. Because of its very weak anomalous signal (Bijvoet ratio  $\cong$  0.6%), Glucose Isomerase is known as a particularly difficult target for sulfur-SAD phasing, especially with Cu radiation. Figure 9 displays the experimental electron density map from data collected with a rotating anode generator and CCD detector<sup>13</sup>. Of the 388 residues, 383 were identified using Arp/wArp.

Figure 8 - Structure solved by SAD phasing

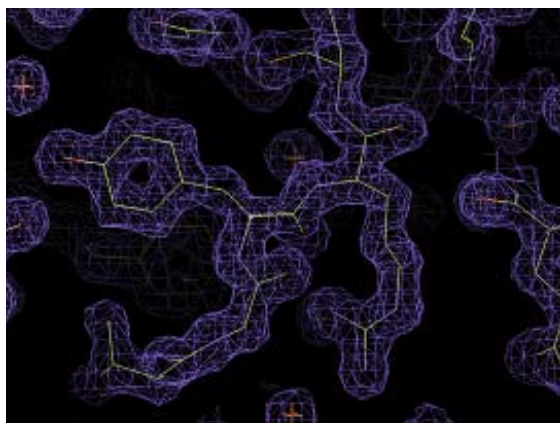


Structure of Glucose Isomerase solved by SAD phasing based on the native sulfur anomalous signal in the home lab using a Bruker CCD. Data were collected to 2.1 Å ( $R_{\text{merge}}=5.7\%$ ) with 31 fold redundancy using an exposure time of 80 sec/deg and rotation angle of 0.5 deg. Phases were calculated from 8 sulfur sites at 2.6 Å and extended out to 2.1 Å using density modification. The data collection was completed in 40 hrs.

Normally with sulfur SAD phasing, at least 15-fold redundancy is required for the experiment to be successful. Obviously, to achieve this same redundancy with an Image Plate would require a much longer experiment.

If a crystal has a high sulfur content, diffracts strongly and the data quality is excellent, sulfur SAD experiments can be successful even with low redundancy. Figure 9 shows a structure of Aldose Reductase solved via SAD phasing of native sulfur in the home lab<sup>14</sup>. The data were collected to 1.6 Å resolution in 16 hours. Even though the crystal system is monoclinic and the redundancy was only 6-fold, the data produced an experimental map that was easy to interpret.

**Figure 9 - Structure of Aldose Reductase**



Structure of Aldose Reductase (34 kDal, 7 Cystines, 6 methionines, no disulphide bridges) solved by SAD phasing from the native sulfur signal. Data were collected with a Bruker CCD detector. 1.6 Å data set, 16 sec/degree, 6-fold redundancy,  $R_{\text{merge}}=3.1\%$ .

## Conclusions

As shown in Table 2, state-of-the-art CCDs now equal or surpass Image Plates in all performance metrics. In particular, because of their higher sensitivity and faster readout CCDs can produce equivalent data in a fraction of the time required by an image plate or, for a given experiment time the CCD can produce significantly superior data quality.

Because of these advantages the CCD is now becoming the preferred detector for a broad range of home laboratory applications from high throughput screening to SAD phasing.

**Table 2**

A comparison of the performance characteristics for Image Plates and CCD detectors. The latest generation of CCDs exhibit significantly superior sensitivity, readout speed and comparable dynamic range and resolving power

	Image Plate	CCD	CCD advantages
Size (mm)	300	100	
Point spread function (FWHM)	200	80	Better spatial resolution allows CCD to work closer to the sample
Resolution at edge of detector	1.63	1.78	
Resolving power (orders)	1500	1300	Because of its smaller point spread function the CCD exhibits comparable resolving power despite its smaller physical size
Sensitivity (DQE)	0.1-0.25	0.5-0.75	CCD more than three times more sensitive
Readout time	60-120 sec	<1 sec	CCD readout 100 times faster, allows fine $\phi$ slicing, high redundancy
Dynamic range	$<10^6$	$10^6$ *	CCDs can now achieve dynamic range comparable to Image plates

\*Intrinsic dynamic range  $5 \times 10^4$ ,  $10^6$  with software rescan.

## References

- <sup>1</sup> J. Miyahara, K. Takahashi, Y. Ameniya, N. Kamiya and Y. Satoh, Nucl. Instrum. Methods, A246, 572 (1986).
- <sup>2</sup> S. Gruner, M.W. Tate, E.F. Eikenberry, Rev. Sci. Instrum. 73(8), 2815 (2002).
- <sup>3</sup> S.W. Muchmore, S.W., Acta Cryst. D55, 1669-1671. (1999).
- <sup>4</sup> I. Naday, E.M. Westbrook, M.L. Westbrook, D.J. Travis, M. Stanton, W.C. Phillips, and J. Xie, Nucl. Instrum. and Meth. A348, 635-640 (1994).
- <sup>5</sup> M. Stanton, W.C. Phillips, D. O'Mara, I. Naday, and E.M. Westbrook, Nucl. Instrum. and Meth. A325, 558-567 (1993).
- <sup>6</sup> M. Thoms, Nucl. Instrum. and Meth. A378, 598-611 (1996).
- <sup>7</sup> J.A. Rowlands, Phys. Med. Biol., R123-166 (2002).
- <sup>8</sup> C. Nave, Acta Cryst. D55, 1663-1668. (1999).
- <sup>9</sup> C. Hall, R. Lewis, Nucl. Instrum. and Meth. A348, 627-630 (1994).
- <sup>10</sup> A. Deacon, T. Gleichmann, S.J. Harrop, J.R. Helliwell, A.J. Kalb and J. Yariv, Rev. Sci. Instrum., 69(9), 3366 (1996).
- <sup>11</sup> J. Howe, D.M. Chambers, C. Courtois, E. Forster, C.D. Gregory, I.M. Hall, O. Renner, I. Ushmann, N.C. Woolsey, Rev. Sci. Instrum., 77, 1-4 (2006)
- <sup>12</sup> R. Schulz-Wendtland, U. Aichinger, M. Sabel, C. Bohner, M. Dobritz, E. Wenkel, W. Bautz, Rontgenpraxis 54(4), 123-126 (2001).
- <sup>13</sup> Lowe, E., Garman, E., et al, in preparation.
- <sup>14</sup> Schierbeek, B., Coetzee, A., Bruker AXS, Lab Report SCD 6.

## Author

Roger Durst, Bruker AXS Inc.



All configurations and specifications are subject to change without notice. Order No. T86-EXS001 © 2007 BRUKER AXS INC. Printed in the U.S.A.

● **Bruker AXS Inc**

5465 East Cheryl Parkway  
Madison, WI 53711 - USA  
Phone +1 (800) 234-XRAY  
Phone +1 (608) 276-3000  
Fax +1 (608) 276-3006  
info@bruker-axs.com  
www.bruker-axs.com

**Bruker AXS GmbH**

Östliche Rheinbrückenstr. 49  
D-76181 Karlsruhe, Germany  
Phone +1 (49) 721 595 2888  
Fax +1 (49) 721 595 4587  
info@bruker-axs.de  
www.bruker-axs.de

**Bruker AXS BV**

Oostsingel 209  
2612 HL Delft, The Netherlands  
Phone +1 (31) 152 152 400  
Fax +1 (31) 152 152 500  
info@bruker-axs.nl  
www.bruker-axs.nl